NOTES AND CORRESPONDENCE

An Approximating Polynomial for the Computation of Saturation Vapor Pressure

PAUL R. LOWE

Naval Environmental Prediction Research Facility, Monterey, Calif. 93940

12 April 1976

ABSTRACT

A procedure for computing saturation vapor by means of a polynomial approximation is presented and evaluated against other methods currently in use. The polynomial procedure is demonstrated to be highly accurate and more economic of computational time requirements than other procedures.

In the many numerical models of atmospheric phenomena which take into consideration the thermodynamics of moist air, it is routinely required to determine values of saturation vapor pressure (and/or actual ambient vapor pressure) one or more times at each grid point of a two- or three-dimensional computational domain at every iteration. Many other types of meteorological calculations also require a determination of this parameter (the compilation of a climatology of atmospheric refractive indices using a large data base, for example). If any meteorological variable deserves to be called ubiquitous, vapor pressure is certainly a leading candidate for the title.

A useful algorithm for calculating any variable must meet two essential criteria. First, the algorithm must be accurate within certain preestablished limits. Ideally values produced by such procedures should conform as closely as possible to some universally accepted standard. The standard in this case is normally taken to be the set of values produced by the Goff-Gratch formulations (List, 1958). Second, the desired procedure should expend as little time as possible, without sacrificing necessary accuracy, when implemented on a digital computer.

A brief review of literature and notes revealed 11 different procedures for computing vapor pressure. These can be divided into two basic categories: those that require exponentiation and those that take the form of a polynomial. In general, the requirement to do an exponentiation (whether the base is e or 10) violates the criterion of economy of computing time. On the other hand, polynomial-type procedures characteristically have been inaccurate.

This note describes a polynomial procedure that consumes a minimal amount of time without sacrificing acceptable accuracy with respect to the standard.

An examination of the curves of saturation vapor pressure indicates that because of their smooth variability with changing temperature they are amenable to approximation by some order of polynomial. A Chebyshev fitting procedure was applied to values of vapor pressure for the temperature range from -50 to $+50$°C for the water reference and -50 to 0°C for the ice reference. A pair of sixth-order polynomials that produced an error of much less than 1% over these ranges was derived. Only the polynomial for the water reference is considered here.

The polynomials take the form

$$E_s = a_0 + T(a_1 + T(a_2 + T(a_3 + T(a_4 + T(a_5 + a_6 T))))), \quad (1)$$

where E_s is saturation vapor pressure (mb), T the temperature in [°C or K (see below)], and the a_i ($i = 0, 1, \ldots, 6$) indicate the numerical coefficients for each term of the polynomial. The polynomial coefficients for the water reference formula are as follows:

Temperatures (°C)	Temperatures (K)
$a_0 = 6.107799961$	$a_0 = 6984.505294$
$a_1 = 4.436518521 \times 10^{-1}$	$a_1 = -188.9039310$
$a_2 = 1.428945805 \times 10^{-2}$	$a_2 = 2.133357675$
$a_3 = 2.650648471 \times 10^{-4}$	$a_3 = -1.288580973 \times 10^{-2}$
$a_4 = 3.031240396 \times 10^{-6}$	$a_4 = 4.393587233 \times 10^{-5}$
$a_5 = 2.034080948 \times 10^{-8}$	$a_5 = -8.023923082 \times 10^{-8}$
$a_6 = 6.136820929 \times 10^{-11}$	$a_6 = 6.136820929 \times 10^{-11}$.

It should be noted that the nested formulation shown in Eq. (1), when used instead of the usual algebraic representation

$$E_s = a_0 + a_1 T + a_2 T^2 + a_3 T^3 + a_4 T^4 + a_5 T^5 + a_6 T^6, \quad (2)$$

is responsible for a significant gain in computational speed.

The values produced by application of Eq. (1) are shown in Column (b) of Table 1 for the range of temperatures indicated. Values produced from a number of other procedures are also shown in Table 1 for comparison. Column (a) shows the Goff-Gratch values (Goff and Gratch, 1946) that are used as the standards of comparison or "bench marks." Columns (c) and (d) give the values resulting from the formulas of Tabata (1973), which are

$$\log_{10}E_2=9.28603523-2.32237885\ (10^3/\theta), \quad (3)$$

$$\log_{10}E_s=8.42926609-1.82717843\ (10^3/\theta) -0.071208271\ (10^3/\theta)^2, \quad (4)$$

where $\theta=T+273.15$, where T is temperature (°C). Column (e) shows values given by the Tetens formula as expressed by Haurwitz (1945) and Murray (1967). These procedures are given by Eqs. (5) and (6):

$$E_s=6.1078\times10^{\mu T/(T+v)}, \quad (5)$$

where T is temperature (°C), $\mu=7.5$ and $v=237.3$; and

$$E_s=6.1078\exp\left[\frac{a(T-273.16)}{T-b}\right], \quad (6)$$

where T is temperature (K), $a=17.2693882$ and $b=35.86$. (Note that both Eqs. (5) and (6) are with reference to liquid water, as are all of the algorithms discussed.)

Column (f) of Table 1 shows the values of Richards' procedure which was described by Wigley (1974). This formula is given by

$$E_s=1013.25\exp(13.3185T-1.9760T^2 -0.6445T^3-0.1299T^4), \quad (7)$$

where $T=1-(\theta_s/\theta)$ and $\theta_s=373.16$ K (the steam point), and θ is temperature (K). It should be noted that Eq. (7) was reformulated for testing so that the polynomial appearing as the exponent was rearranged into a nested form similar to that of (1).

The bottom three rows of Table 1 (data expressed as percentages) show values of the root-mean-square (rms) percentage error,

$$\epsilon=\left[\frac{(E_G-\tilde{E})^2}{N}\right]^{\frac{1}{2}}, \quad (8)$$

where E_G is the Goff-Gratch standard value and $\tilde{E}$ is the value produced by the appropriate algorithm. Mean percentage errors are given for the total range of temperatures as well as for the ranges of −15 to 50°C and 0 to 35°C. Values shown in parentheses are individual percentage errors.

Table 1 gives a good picture of comparative accuracy, but as noted earlier, computing time must also be considered. Fig. 1 shows the efficiencies of the various procedures in terms of both accuracy and computing time. The vertical coordinate represents accuracy in terms of the rms percentage error and the horizontal coordinate shows time requirements in terms of seconds per computation. Fig. 1 demonstrates efficiency for the three temperature ranges (−50 to +50°C, −15 to 50°C and 0 to 35°C). Com-

TABLE 1. Values of saturation vapor pressure for the temperature range −50 to 50°C produced by the application of Eq. (1), with values produced by other accepted procedures provided for comparison.

Values (individual mean percentage errors shown in parentheses)												
(a) Goff-Gratch		(b) Lowe		(c) Tabata I		(d) Tabata II		(e) Tetens		(f) Richards		
−50	0.06356	0.06337	(−0.29)	.07564	(19.006)	.06474	(1.856)	.06078	(−4.400)	.06361	(0.080)	
−45	0.11114	0.11170	(0.54)	.12790	(15.080)	.11287	(1.556)	.10735	(−3.400)	.11111	(−0.026)	
−40	0.18914	0.18915	(0.03)	.21142	(11.780)	.19459	(1.295)	.18423	(−2.600)	.18900	(−0.074)	
−35	0.31387	0.31314	(−0.24)	.34220	(9.026)	.31721	(1.064)	.30783	(−1.900)	.31360	(−0.087)	
−30	0.50880	0.50777	(−0.20)	.54302	(6.725)	.51312	(0.849)	.50177	(−1.380)	.50839	(−0.080)	
−25	0.80697	0.80620	(−0.10)	.84579	(4.810)	.81223	(0.652)	.79928	(−0.95)	.80645	(−0.064)	
−20	1.25401	1.25386	(−0.01)	1.29453	(3.260)	1.25992	(0.471)	1.24622	(−0.62)	1.25344	(−0.045)	
−15	1.91178	1.91226	(0.02)	1.94893	(1.1943)	1.91763	(0.306)	1.90463	(−0.37)	1.91126	(−0.027)	
−10	2.86270	2.86350	(0.028)	2.88889	(0.915)	2.86728	(0.160)	2.85709	(−0.196)	2.86237	(−0.012)	
− 5	4.21485	4.21548	(0.016)	4.21978	(0.002)	4.21630	(0.034)	4.21168	(−0.075)	4.21486	(0.00)	
0	6.1078	6.1078	(0.00)	6.07889	(−0.473)	6.1036	(−0.069)	6.1078	(0.00)	6.10829	(0.008)	
5	8.71922	8.71839	(−0.009)	8.64290	(−0.875)	8.7063	(−0.148)	8.72272	(0.04)	8.72028	(0.012)	
10	12.2723	12.2707	(−0.010)	12.1366	(−1.106)	12.2476	(−0.201)	12.2789	(0.054)	12.27392	(0.013)	
15	17.0438	17.0419	(−0.012)	16.8429	(−1.179)	17.0052	(−0.226)	17.0523	(0.05)	17.04585	(0.012)	
20	23.3730	23.3712	(−0.008)	23.1144	(−1.106)	23.3207	(−0.224)	23.3810	(0.034)	23.37507	(0.009)	
25	31.6709	31.6693	(−0.005)	31.3862	(−0.899)	31.6102	(−0.192)	31.6749	(0.013)	31.67243	(0.005)	
30	42.4304	42.4289	(−0.002)	42.1901	(−0.566)	42.3752	(−0.130)	42.4264	(−0.009)	42.43055	(0.001)	
35	56.2366	56.2348	(−0.002)	56.1713	(−0.116)	56.2149	(−0.038)	56.2206	(−0.028)	56.2341	(−0.004)	
40	73.7775	73.7754	(−0.002)	74.1052	(0.444)	73.8385	(0.083)	73.7473	(−0.041)	73.77157	(−0.008)	
45	95.8548	95.8553	(0.000)	96.9171	(1.108)	96.0787	(0.234)	95.8125	(−0.044)	95.84413	(−0.011)	
50	123.4	123.408	(0.006)	125.7029	(1.866)	123.9055	(0.410)	123.351	(−0.036)	123.37879	(−0.013)	
Root-Mean-Square Error (expressed in percentages)												
−50°C − +50°C		0.152		6.559		0.711		1.459		0.040		
−15°C − +50°C		0.012		0.949		0.202		0.118		0.012		
0 − +35°C		0.007		0.864		0.167		0.034		0.009		

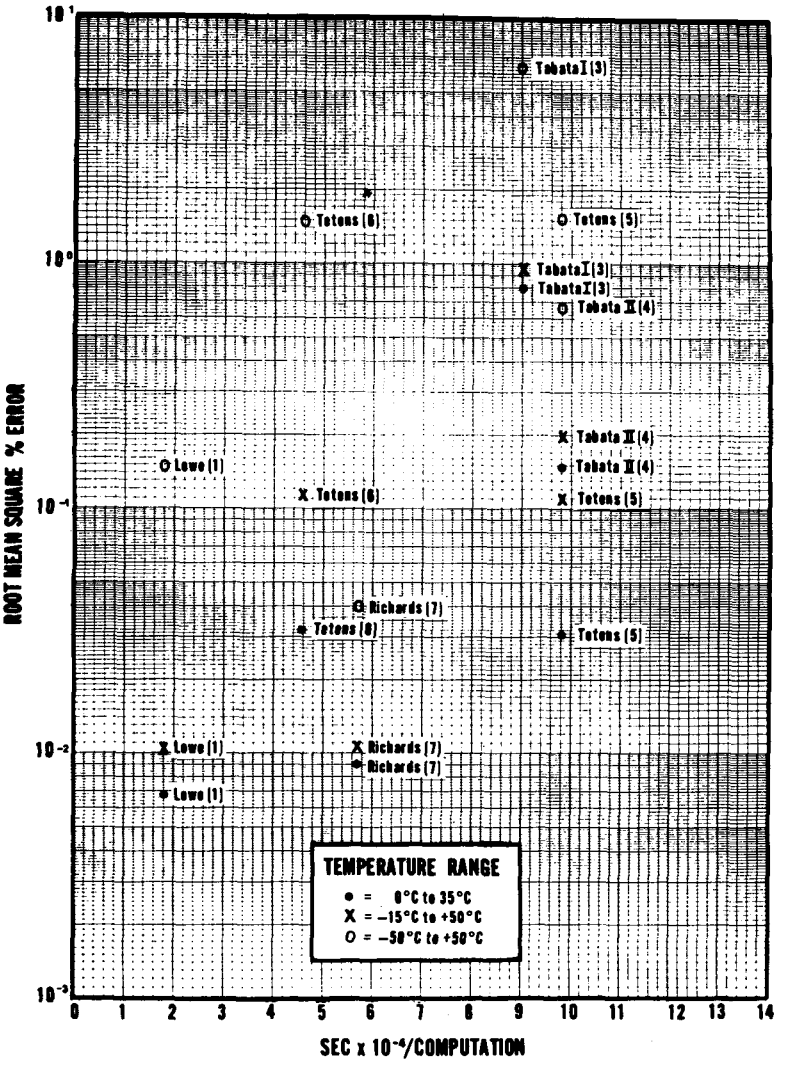

FIG. 1. Computing speed vs accuracy for vapor pressure algorithms for temperature ranges 0 to 35°C, −15 to 50°C and −50 to 50°C. Numbers in parentheses reference equations in text.

puting times are for a CDC-3100 system using FORTRAN. Checks on larger, faster machines indidicate that the relative values hold and are computer-independent.

These plots show that with the exception of the Richards procedure (and then only when the very low part of the temperature range is considered), the polynomial procedure is considerably closer in value to the Goff-Gratch values than the others. Also, for the two temperature ranges of greater meteorological significance, the polynomial procedure is as accurate as Richards. Further, the polynomial is approximately three times faster regardless of range.

As Murray (1967) has shown, saturation vapor pressure values determined by Eq. (6) depart from the standard by amounts less than the degree of uncertainty embodied in the standard. The polynomial (and the Richards) values, which have even smaller departures, must be further within the zone of uncertainty.

The polynomial algorithm clearly meets both criteria (accuracy and economy of computing time) for use in numerical modelling, and is therefore recommended for such use.

Similar polynomials exist for approximating saturation vapor pressure with respect to ice and also for determining the derivatives of E_s with respect to temperature for both water and ice reference (Lowe and Ficke, 1974). These polynomials are also of the sixth order and take the form of Eq. (1). The appropriate coefficients, given temperatures in °C, are

as follows:

E_s (ice)	dE_s/dT (water)	dE_s/dT (ice)
$a_0=6.109177956$	$a_0=4.438099984\times10^{-1}$	$a_0=5.030305237\times10^{-1}$
$a_1=5.03469897\times10^{-1}$	$a_1=2.857002636\times10^{-2}$	$a_1=3.773255020\times10^{-2}$
$a_2=1.886013408\times10^{-2}$	$a_2=7.938054040\times10^{-4}$	$a_2=1.267995369\times10^{-3}$
$a_3=4.176223716\times10^{-4}$	$a_3=1.215215065\times10^{-5}$	$a_3=2.477563108\times10^{-5}$
$a_4=5.824720280\times10^{-6}$	$a_4=1.036561403\times10^{-7}$	$a_4=3.005693132\times10^{-7}$
$a_5=4.838803174\times10^{-8}$	$a_5=3.532421810\times10^{-10}$	$a_5=2.158542548\times10^{-9}$
$a_6=1.838826904\times10^{-10}$	$a_6=-7.090244804\times10^{-13}$	$a_6=7.131097725\times10^{-12}$.

The temperature ranges are −50 to 50°C for water reference and −50 to 0°C for ice references. The errors for these algorithms over their appropriate ranges are well within 1% except for dE_s/dT at −45 to −50°C, where the error is approximately 1%.

REFERENCES

Goff, J. A., and S. Gratch, 1946: Low-pressure properties of water from −160 to 212°F. *Trans. ASHVE*, 52, 95–121.

Haurwitz, B., 1945: *Dynamic Meteorology*. McGraw-Hill, 365 pp.

List, R. J., 1958: *Smithsonian Meteorological Tables*, 6th rev. ed. The Smithsonian Institution, 527 pp.

Lowe, P. R., and J. M. Ficke, 1974: The computation of saturation vapor pressure. ENVPREDRSCHFAC Tech. Pap. 4–74, Environmental Prediction Research Facility, Monterey, Calf., 27 pp.

Murray, F. W., 1967: On the computation of saturation vapor pressure. *J. Appl. Meteor.*, 6, 203–204.

Tabata, S., 1973: A simple but accurate formula for the saturation vapor pressure over liquid water. *J. Appl. Meteor.*, 12, 1410–1411.

Wigley, T. M. L., 1974: Comments on "A simple but accurate formula for the saturation vapor pressure over liquid water," 3, *J. Appl. Meteor.*, 13, 608.

Seasonal and Wavelength Dependence of Urban/Rural Radiance in Iowa

B. K. LUNDE

Department of Aerospace Engineering, Iowa State University, Ames, and Brooks Borg and Skiles, Architects-Engineers, Des Moines 50309

5 January 1976 and 9 December 1976

ABSTRACT

LANDSAT measurements show that the radiance of urban areas is higher in the summer than that of rural areas and lower in the winter, aiding the heat budget of cities and tending to save energy. The radiance of both urban and rural areas increases with snow cover in winter, but cities have less radiance than the country. In the early summer the country has low radiance in the near infrared, and in the late summer it has low radiance in the visible region of the spectrum; the radiance of urban areas follows these trends in a very limited way.

1. Introduction

There has been extensive work worldwide on urban climate (Chandler, 1970) and some work on measurement of radiance on a larger than planetary scale (Nordberg *et al.*, 1962; Bray and Archer, 1966); however, recent work on the heat budget (Critchfield, 1974) of cities (Atwater, 1975) has used the same albedo value for rural, suburban and urban areas for summer and winter seasons. The present work was started because of the striking appearance of cities on LANDSAT imagery and the apparent reversal from summer to winter data shown in Fig. 1. Note in Fig. 1a that cities are lighter than the rural areas, while in Fig. 1b cities are darker. This reversal indicates a significant beneficial factor in urban heat budgets due to the variation of radiance between urban and rural areas.

2. Discussion

LANDSAT 1 and LANDSAT 2 are spacecraft designed to acquire multispectral images of the earth's surface. They pass each local area across most of the